Field dependences of surface magnetization in a semi-infinite Ising model with a nonrandom surface or surface amorphization

T. Kaneyoshi
Department of Physics, Nagoya University, 464 Nagoya, Japan
(Received 21 July 1988; revised manuscript received 25 October 1988)

Field dependences of surface magnetization in the semi-infinite spin-$\frac{1}{2}$ Ising ferromagnet with a nonrandom surface or surface amorphization are investigated by the use of the effective-field theory corresponding to the Zernike approximation in the bulk. We find that the system behaves in a variety of notable ways for both the random and the uniform models.

I. INTRODUCTION

The problems of surface magnetism have been investigated for many years. In particular, the semi-infinite simple cubic spin-$\frac{1}{2}$ Ising ferromagnet with a (100) uniform surface has received much attention and has been studied by using a variety of approximations and mathematical techniques.[1-7] For this simple model with modified exchange interaction J_s only at the surface, it was pointed out, on the basis of the standard mean-field approximation,[1] that for J_s greater than a critical value J_s^c, the system could order on the surface before it ordered in the bulk. Since then, a number of authors have investigated the possibility of the surface magnetic phase. This mean-field prediction is now found to be qualitatively correct. This phase is characterized by a surface Curie temperature higher than that of the bulk. Experimentally, surface magnetic order has been exhibited mainly in crystalline systems such as Ni, Cr, and Gd.[4]

The temperature dependence of magnetization at the surface have also been investigated experimentally and theoretically. They show some characteristic behaviors. For instance, linear temperature dependence of surface magnetization has been observed in the temperature region near the bulk transition temperature when J_s is taken as a value smaller than J_s^c.[4,8] However, as far as we know, the magnetic field dependence of magnetization at the surface has not been examined.

On the other hand, in the previous work[9] we have investigated the phase diagrams and magnetizations of the semi-infinite spin-$\frac{1}{2}$ Ising ferromagnet with surface amorphization by the use of the effective-field theory corresponding to the Zernike approximation in the bulk.[7] We found a number of characteristic behaviors for the surface magnetic properties, such as the possibility of surface reentrant phenomena, and proposed that research on a surface with an amorphous layer may open a new field of surface magnetism.

The purpose of this work is to study the field dependences (or magnetization processes) of surface magnetization in the semi-infinite simple cubic spin-$\frac{1}{2}$ Ising ferromagnet with a (100) uniform surface or surface amorphization within the same framework as that of the previous work.[7,9] We find some characteristic behaviors for the magnetization processes of surface and bulk magnetizations in the system with a uniform surface, depending on whether J_s is larger (or smaller) than a critical value J_s^c. The field dependence of surface magnetization for the system with an amorphous surface layer indicate that the research of the system in an applied field is also extremely interesting.

The outline of this work is as follows. In Sec. II, we present the basic points of the theory. In Sec. III, we examine the field dependences (or magnetization processes) of the surface and bulk magnetizations for the system with a (100) uniform surface. In relation to the results of the previous work, the temperature dependences of surface magnetization for the system with an amorphous surface layer are investigated in Sec. IV, changing the value of applied magnetic field.

II. FORMULATION

We consider a semi-infinite spin-$\frac{1}{2}$ Ising ferromagnet with a (100) uniform surface or surface amorphization. The Hamiltonian is given by

$$\mathcal{H}=-\tfrac{1}{2}\sum_{i,j}J_{ij}S_i^zS_j^z-H\sum_i S_i^z\ , \tag{1}$$

where the summation is carried out only over nearest-neighbor pairs of spins. S_i^z takes the values ± 1. J_{ij} is the exchange interaction, which takes the value $\bar{J}_s$ if both i and j sites belong to the (100) surface, $\bar{J}_1$ between spins on the surface and its nearest neighbor at the first layer, and the bulk interaction J otherwise. H is the external field. For the surface amorphization, $\bar{J}_s$ and $\bar{J}_i$ are assumed to be randomly distributed according to the independent probability distribution functions $P(\bar{J}_s)$ and $P(\bar{J}_1)$. For the uniform surface, on the other hand, $\bar{J}_s$ and $\bar{J}_1$ are taken as the fixed values J_s and J_1.

In the following, we assume that the site magnetizations $\sigma_i=\langle S_i^z\rangle$, where $\langle\cdots\rangle$ denotes the canonical average are equivalent to each other on a layer for the layered simple cubic system with a (100) surface. As discussed in the previous works,[7,9] when we apply the effective-field theory with correlations to our layered system, the surface magnetization σ_s after performing the random-bond average, is given by

 ©1989 The American Physical Society

$$\sigma_s=[\langle\cosh(D\bar{J}_s)\rangle_r+\sigma_s\langle\sinh(D\bar{J}_s)\rangle_r]^4 \times[\langle\cosh(D\bar{J}_1)\rangle_r+\sigma_1\langle\sinh(D\bar{J}_1)\rangle_r]f(x)|_{x=0} , \quad (2)$$

with

$$f(x)=\tanh[\beta(x+H)] , \quad (3)$$

where $\beta=1/k_BT$, $D=\partial/\partial x$ is a differential operator, and $\langle\cdots\rangle_r$ represents the random-bond average. For the magnetization σ_1 of the first (next) layer, we have

$$\sigma_1=[\cosh(DJ)+\sigma_1\sinh(DJ)]^4 \times[\langle\cosh(D\bar{J}_1)\rangle_r+\sigma_s\langle\sinh(D\bar{J}_1)\rangle_r] \times[\cosh(DJ)+\sigma_2\sinh(DJ)]f(x)|_{x=0} . \quad (4)$$

In general, the magnetization σ_n of the nth layer is given by

$$\sigma_n=[\cosh(DJ)+\sigma_n\sinh(DJ)]^4 \times[\cosh(DJ)+\sigma_{n-1}\sinh(DJ)] \times[\cosh(DJ)+\sigma_{n+1}\sinh(DJ)]f(x)|_{x=0} \text{ for } n\geq 2 , \quad (5)$$

where σ_{n-1} and σ_{n+1} are the magnetizations in the $(n-1)$th and $(n+1)$th layers, respectively.

Expanding the right-hand sides of (2), (4), and (5), we obtain the following set of coupled equations:

$$\sigma_s=A_1+4A_2\sigma_s+6A_3\sigma_s^2+4A_4\sigma_s^3+A_5\sigma_s^4 +\sigma_1(A_6+4A_7\sigma_s+6A_8\sigma_s^2+4A_9\sigma_s^3+A_{10}\sigma_s^4) , \quad (6)$$

$$\sigma_1=B_1+4B_2\sigma_1+6B_3\sigma_1^2+4B_4\sigma_1^3+B_5\sigma_1^4 +\sigma_s(B_7+4B_8\sigma_1+6B_9\sigma_1^2+4B_{10}\sigma_1^3+B_{11}\sigma_1^4) +\sigma_2(B_2+4B_3\sigma_1+6B_4\sigma_1^2+4B_5\sigma_1^3+B_6\sigma_1^4) +\sigma_s\sigma_2(B_8+4B_9\sigma_1+6B_{10}\sigma_1^2+4B_{11}\sigma_1^3+B_{12}\sigma_1^4) , \quad (7)$$

and

$$\sigma_n=K_1+4K_2\sigma_n+6K_3\sigma_n^2+4K_4\sigma_n^3+K_5\sigma_n^4+(\sigma_{n-1}+\sigma_{n+1})(K_2+4K_3\sigma_n+6K_4\sigma_n^2+4K_4\sigma_n^3+K_6\sigma_n^4) +\sigma_{n+1}\sigma_{n-1}(K_3+4K_4\sigma_n+6K_5\sigma_n^2+4K_6\sigma_n^3+K_7\sigma_n^4) , \quad (8)$$

where coefficients A_i $(i=1-10)$, B_i $(i=1-12)$, and K_i $(i=1-7)$ are given in the Appendix. When $H=0$, these equations reduce to those in Ref. 9 [namely Eqs. (16), (17), and (18) of Ref. 9.]

We are unable to solve the above coupled equations analytically. Even if we use a numerical method, they must be terminated at a certain layer. As discussed in previous work,[7,9,10] the simplest method for solving them is to assume that the magnetization remains unaltered after the second layer, namely,

$$\sigma_2=\sigma_3=\cdots=\sigma_n=\sigma_B ,$$

where σ_B is the bulk magnetization determined from

$$\sigma_B=K_1+6K_2\sigma_B+15K_3\sigma_B^2+20K_4\sigma_B^3 +15K_5\sigma_B^4+6K_6\sigma_B^5+K_7\sigma_B^6 . \quad (9)$$

The approximation may be called the three-layer approximation. As shown in the previous works,[7,9,10] the three-layer approximation gives a rather reasonable result for the zero-field ($H=0$) thermal behavior of σ_s except in the temperature region very near $T=T_c^b$ (or T_c^s), where T_c^b (or T_c^s) is the bulk transition temperature (or the surface ordering temperature). In the following, let us use the three-layer approximation to evaluate the field dependences of σ_s and σ_B as a whole.

III. NONRANDOM SURFACE

In this section, we at first investigate the field dependences of σ_s and σ_B for the system with a (100) nonrandom surface. Then, the exchange interactions $\bar{J}_s$ and $\bar{J}_1$ are given by constant values J_s and J_1. Before showing the numerical results, it is worth mentioning that the phase diagram of the present system with $H=0$ has been investigated in previous work.[7] The surface exchange interaction J_s is scaled with that of bulk in the form

$$J_s=J(1+\Delta_s) \quad (10)$$

In the model with $J_1=J$ (Mills's model), it is well known that if the parameter Δ_s is greater than a critical value Δ_c, the system may order on the surface before it orders in the bulk. The system exhibits two successive transitions, namely the surface and bulk phase transitions, as the temperature is lowered. If the ratio is less than Δ_c, the system becomes ordered at the bulk transition temperature. Within the present formulation, the critical value Δ_c is given by $\Delta_c=0.3068$, as discussed in previous work.[7] The value can be compared with $\Delta_c=0.25$ for the mean-field theory,[1] $\Delta_c=0.6$ for the high-temperature series-expansion method,[2] $\Delta_c=0.307$ for the renormalization-group approach,[5] and $\Delta_c=0.5$ for the Monte Carlo method.[3]

In particular, for $H=0$, the bulk equation (9) reduces

to

$$\sigma_B = 6K_2\sigma_B + 20K_4\sigma_B^3 + 6K_5\sigma_B^5 , \quad (11)$$

from which the bulk transition temperature T_c^b can be determined from

$$6K_2 = 1 ,$$

or

$$\tanh(6\beta J) + 4\tanh(4\beta J) + 5\tanh(2\beta J) = \tfrac{16}{3} . \quad (12)$$

The equation (12) is equivalent to that obtained by Zernike,[11] using another method. Then, T_c^b is given by $k_B T_c^b = 5.073$ J, which can be compared with $k_B T_c^b = 6$ J for the mean-field theory result, $k_B T_c^b = 4.933$ J for the Bethe-Peierls approximation result and $k_B T_c^b = 4.511$ J for the high-temperature-expansion-method[12] result.

Figure 1 shows the temperature dependences of σ_s and σ_B for the system with $J_s = J$ and $J_1 = J$, when the value of H is changed. Solid and dashed lines represent σ_s and σ_B, respectively. As mentioned above, the surface for $H = 0$ can order at $T = T_c^b$, since the system satisfies the condition $\Delta_s < \Delta_c$. As is seen from the figure, the magnetization curve σ_s for $H = 0$ [solid curve labeled (a)] changes linearly with T. Experimentally, such a linear temperature dependence of σ_s has been observed in many semi-infinite crystalline magnets.[4]

In Fig. 2, the magnetization processes for the system of Fig. 1 are plotted for the selected values of T, namely $k_B T = 4.0$ J, $k_B T = k_B T_c^b = 5.073$ J, and $k_B T = 6.0$ J. Solid and dashed lines represent σ_s and σ_B, respectively. The magnetization process of σ_B is always above the corresponding curve of σ_s for the whole range of H.

Figure 3 shows the temperature dependences of σ_s for

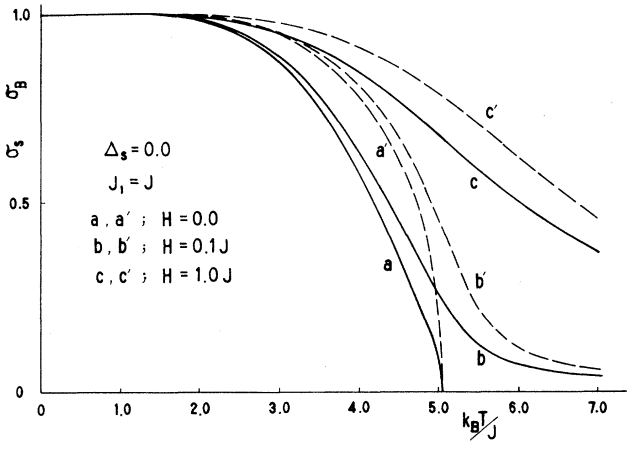

FIG. 1. Temperature dependences of surface and bulk magnetizations for the system with a (100) uniform surface, when the value of H is changed; The curves (a) and (a') are obtained for $H = 0$. (b) and (b') are plotted for $H = 0.1J$. (c) and (c') are for $H = J$. The parameters Δ_s and J_1 are then taken as $\Delta_s = 0.0$ and $J_1 = J$. The solid and dashed lines represent the surface and bulk magnetizations.

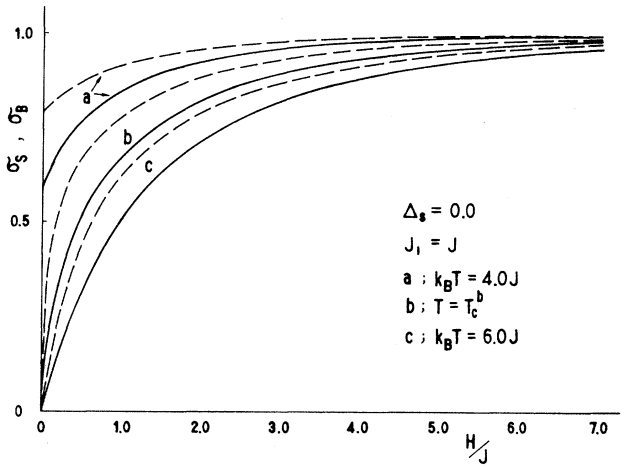

FIG. 2. Magnetization processes of σ_s and σ_B for the system of Fig. 1 at some selected temperatures; the curves (a), (b), and (c) are plotted for $k_B T = 4.0$ J, $T = T_c^b$, and $k_B T = 6.0$ J, respectively. Solid and dashed lines represent, respectively, σ_s and σ_B.

the system with $J_1 = J$ in some applied fields, when Δ_s is taken as $\Delta_s = 1.0$. Since Δ_s is larger than the critical value Δ_c, surface magnetization may take a finite value even in the temperature range above $T = T_c^b$, as is seen from the solid curve (a) with $H = 0$ in the figure. Then, the solid curve (a) exhibits a small dip at $T = T_c^b$. However, when the applied field takes a finite value, such a dip disappears in the magnetization curve of σ_s. The dashed line expresses the σ_B curve for $H = 0$.

In Fig. 4, the magnetization processes of σ_s (or σ_B) for

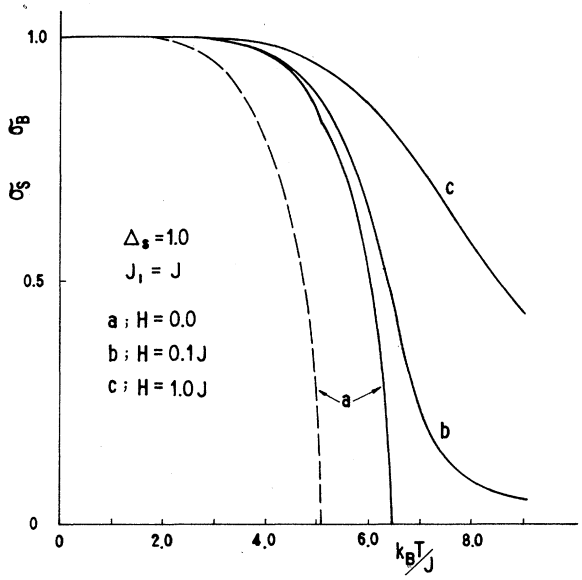

FIG. 3. Temperature dependence of σ_s for the system with $\Delta_s = 1.0$ and $J_1 = J$, when the value of H is changed as follows: (a) $H = 0$, (b) $H = 0.1J$, and (c) $H = J$. The dashed line represents the magnetization curve of σ_B for $H = 0$.

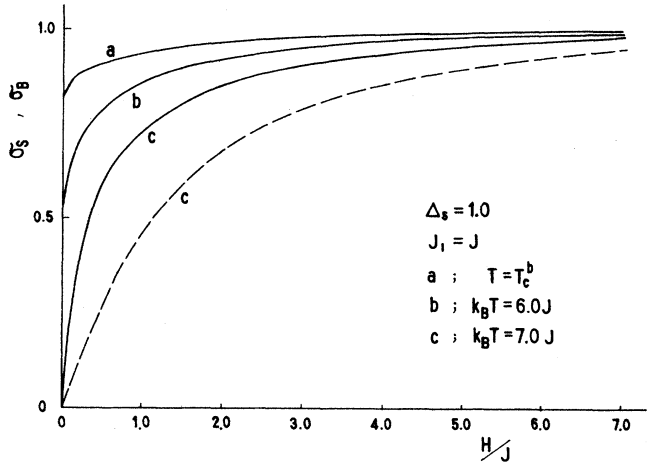

FIG. 4. Magnetization processes of σ_s for the system of Fig. 3 when T is fixed as follows: (a) $T=T_c^b$, (b) $k_BT=6.0$ J, and (c) $k_BT=7.0$ J. The dashed line represents that of σ_B obtained at $k_Bt=7.0$ J.

the system of Fig. 3 are plotted, when the temperature is fixed at $T=T_c^b$ [curve (a)], $K_BT=6.0$ J [curve (b)], and $k_BT=7.0$ J [curve (c)]. The dashed line represents the magnetization process of σ_B at $k_BT=7.0$ J. The magnetization processes of σ_B at $T=T_c^b$ and $k_BT=6.0$ J are equivalent to the dashed curves (b) and (c) in Fig. 2. In contrast with Fig. 2, the magnetization process of σ_s in Fig. 4 is always above the corresponding curve of σ_B for the whole range of H. In particular, the initial rapid rise of the solid curve (a) from the value for $H=0$ comes from the disappearance of the dip seen in the solid curve (a) of Fig. 3.

Figure 5 shows the Arrott plots for the system of Fig. 3 with $\Delta_s=1.0$ and $J_1=J$, when the temperature is fixed at $T=T_c^s$. The T_c^s is given by $k_BT_c^s=6.45$ J from the solid curve (a) of Fig. 3. As is seen from Fig. 5, when the σ_s^2 is plotted by $H/J\sigma_s$, then the solid curve at first increases linearly with H and then exhibits the downward curvature, as is usually observed in the Arrott plots of ferromagnets. On the other hand, when σ_s^2 and σ_B^2 are plotted by $H/J\sigma_B$, they show a bid difference, as shown in the dashed lines. Thus, from the difference the existence of magnetic ordering on the surface may be confirmed.

Figure 6 shows the temperature dependences of σ_s for the system with $\Delta_s=0.0$ and $J_1=0.1J$, when the value of H is changed. The surface is coupled to the first layer by the weak exchange interaction $J_1=0.1J$, so that the surface magnetization [the solid curve (a) with $H=0$] at first follows the two-dimensional bulk magnetization curve [the bulk transition temperature for $z=4$ is given by $k_BT_c^b$ $(z=4)=3.090$ J[13] (where z is the coordination number], takes small values above $T=T_c^b$ $(z=4)$ and is reduced to zero at the bulk transition temperature $k_BT_c^b=5.073$ J. The dashed line represents the bulk magnetization curve σ_B for $H=0$. Comparing Fig. 1 with Fig. 6, the field dependences of σ_s has a form similar to that of Fig. 1.

IV. SURFACE AMORPHIZATION

In the previous work,[9] we have investigated the phase diagrams and the temperature dependences of σ_s and σ_B for the semi-infinite Ising system with a surface amorphization. Experimentally, the surface amorphization can be achieved by using a short laser pulse to melt a thin layer on the surface.[14] Then, we have found a number of interesting phenomena for the thermal behavior of surface magnetization. In this section, let us examine the effects of an applied magnetic field on some surface magnetiza-

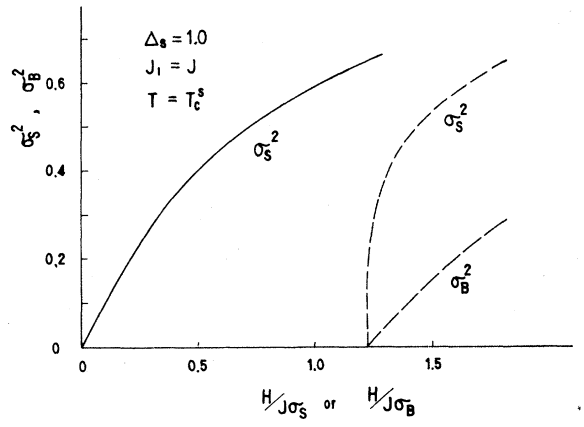

FIG. 5. Arrott plots of σ_s and σ_B for the system with $\Delta_s=1.0$ and $J_1=J$ at the surface ordering temperature $T=T_c^s$, when the vertical axis is plotted by $H/J\sigma_B$. The solid line represents the σ_s^2 vs $H/J\sigma_s$. The dashed lines represent the σ_s^2 (or σ_B^2) vs $H/J\sigma_B$.

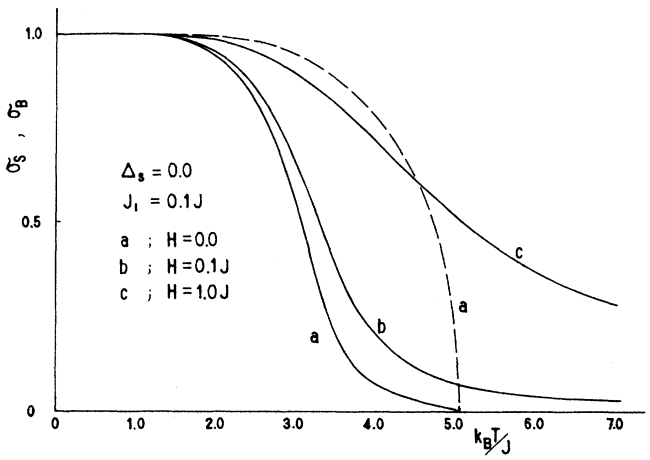

FIG. 6. Temperature dependences of σ_s for the system with $\Delta_s=0.0$ and $J_1=0.1J$, when the value of H is changed as follows. (a) $H=0$, (b) $H=0.1J$ and (c) $H=J$. The dashed line represents the magnetization curve of σ_B for $H=0$.

tion curves, selecting the most interesting cases, such as the surface reentrant phenomenon, from the previous results for $H=0$.

Now, in order to evaluate the random bond averages in (2) and (4), it is necessary to provide the appropriate forms of the probability distribution functions $P(\bar{J}_s)$ and $P(\bar{J}_1)$, describing the structural disorder in a simple way. In the previous work,[9] therefore, we have taken $P(\bar{J}_s)$ and $P(\bar{J}_1)$ as

$$P(\bar{J}_s)=\tfrac{1}{2}[\delta(\bar{J}_s-J_s-\Delta J_s)+\delta(\bar{J}_s-J_s+\Delta J_s)]\ ,$$
$$P(\bar{J}_1)=\tfrac{1}{2}[\delta(\bar{J}_1-J_1-\Delta J_1)+\delta(\bar{J}_1+J_1+\Delta J_1)]\ , \tag{13}$$

as has been done in work on amorphous bulk ferromagnets.[15] The random-bond averages in Eq. (2) and (4) are then given by

$$\langle\cosh(D\bar{J}_\alpha)\rangle_r=\cosh(DJ_\alpha\delta_\alpha)\cosh(DJ_\alpha)\ ,$$
$$\langle\sinh(D\bar{J}_\alpha)\rangle_r=\cosh(DJ_\alpha\delta_\alpha)\sinh(DJ_\alpha)\ \text{for}\ \alpha=s\ \text{or}\ 1\ , \tag{14}$$

where we defined the parameter δ_α as

$$\delta_\alpha=\frac{\Delta J_\alpha}{J_\alpha}\ \text{for}\ \alpha=s\ \text{or}\ 1\ , \tag{15}$$

The result (14) can be also obtained by using the so called "lattice model" of amorphous magnets.[16]

Figure 7 shows the thermal behaviors of σ_s for the system with $\Delta_s=0.0$, $\delta_s=1.2$, and $\delta_1=0.0$ when J_1 is taken as $J_1=0.1J$, changing the value of H. As discussed in the previous work, the curve (a) with $H=0$ exhibits a minimum and a maximum with the increase of T, which corresponds to the trace of the reentrant phenomenon in the two-dimensional frustrated bulk ferromagnet. In fact, for $\delta_s=1.2$, the surface exchange interaction $\bar{J}_s$ can take two values, $\bar{J}_s=2.2J$ and $\bar{J}_s=-0.2J$, with equal probability. If we put $J_1=0$, the surface then reduces to the two-dimensional bulk system (or square lattice), which can exhibit the reentrant phenomenon as well as the spin-glass phase.[17] In Fig. 7, however, the surface is coupled to the first layer by the weak exchange interaction $J_1=0.1J$, so that even for $H=0$ the surface state is similar to that for which a weak magnetic field is applied to the two-dimensional frustrated bulk system. With the increase of H, the curves in Fig. 7 exhibit behavior very similar to those obtained in Ref. 17 for the two-dimensional frustrated bulk system. With the increase of H, the curves in Fig. 7 exhibit behavior very similar to that observed in Ref. 17 for the two-dimensional frustrated bulk system.

When J_s is taken as $J_s=8.0J$ (or $\Delta_s=7.0$), we have found characteristic behavior for the temperature dependence of σ_s in $H=0$; the surface reentrant phenomenon has been obtained in the temperature range above $T=T_c^b$, when J_1 is taken as $J_1=0.1J$. The sharp discontinuity of the derivative of σ_s at $T=T_c^b$ has been observed for the system, when J_1 is taken as $J_1=J$. In Figs. 8 and 9, therefore, we examine the effects of applied magnetic field on σ_s for such systems.

In Fig. 8, the temperature dependences of σ_s are plotted for the system with $J_1=J$, $\delta_s=1.1$, and $\delta_s=0.0$, when the value of H is changed. The dashed line represents the magnetization curve of σ_B for $H=0$. The sharp discontinuity of the derivation of σ_s is observed at $T=T_c^b$ for the curve with $H=0$. With the increase of H, however, such a discontinuity disappears. But, the characteristic behavior of σ_s for $H=0$ remains even for $H=0.5J$.

In Fig. 9, the field dependences of σ_s are investigated for the system with $J_s=8J$, $J_1=0.1J$, $\delta_s=1.1$, and

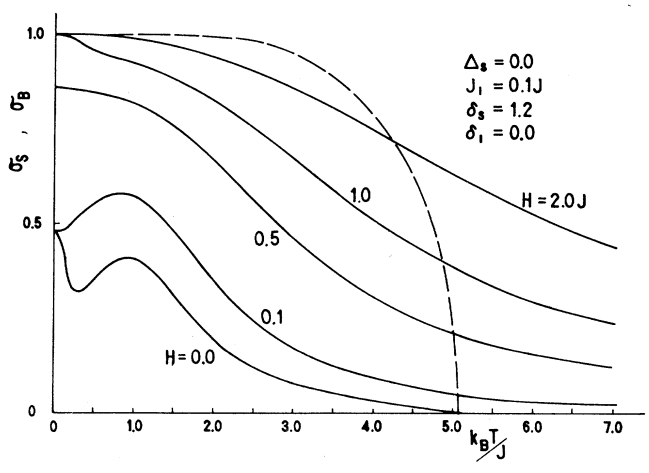

FIG. 7. Temperature dependences of σ_s for the system with a surface amorphization, when the value of H is changed as $H=0.0$, $H=0.1J$, $H=0.5J$, $H=J$, or $H=2.0J$. The parameters Δ_s, J_1, δ_s, and δ_1, are then taken as $\Delta_s=0.0$, $J_1=0.1J$, $\delta_s=1.2$, and $\delta_1=0.0$. The dashed line represents the bulk magnetization σ_s for $H=0$.

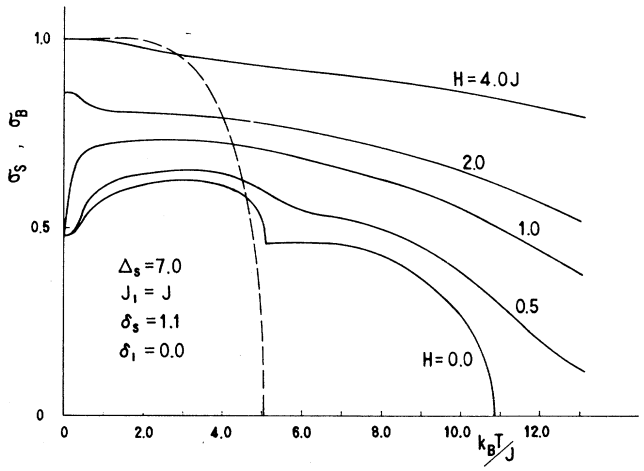

FIG. 8. Temperature dependences of σ_s for the surface amorphization with $\Delta_s=7.0$, $J_1=J$, $\delta_s=1.1$, and $\delta_1=0.0$, when the value of H is changed as $H=0.5J$, $H=J$, or $H=4.0J$. The dashed line represents the σ_B for $H=0$.

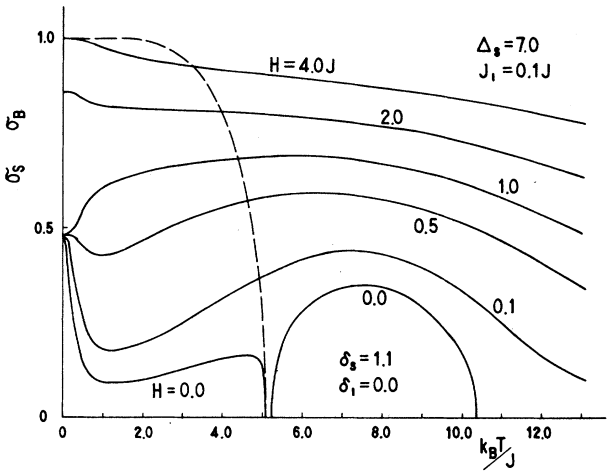

FIG. 9. Temperature dependences of σ_s for the surface amorphization with $\Delta_s=7.0$, $J_1=0.1J$, $\delta_s=1.1$, and $\delta_1=0.0$, when the value of H is changed as $H=0.0$, $H=0.1J$, $H=0.5J$, $H=J$, $H=2.0J$, or $H=4.0J$. The surface-reentrant phenomenon is observed for $H=0.0$. The dashed line represents the σ_B for $H=0.0$.

$\delta_1=0.0$. As is seen in the figure, the surface-reentrant phenomenon is obtained for the case of $H=0$ in the temperature region above $T=T_c^b$, although it does not appear for $J_1=J$, as shown in Fig. 8. The curve with $H=0$ also exhibits a characteristic behavior in the temperature region below $T=T_c^b$; it has finite values and furthermore shows a minimum and a maximum in the region of T. Such a phenomenon comes from the fact that frustrated spins on the surface are coupled to the ferromagnetic layers and are apt to align to the z direction in that temperature range, even if the surface-reentrant phenomenon is observed above $T=T_c^b$. Even for $H=0.1J$, however, the reentrant phenomenon easily disappears, although the characteristic behaviors observed for the curve of σ_s with $H=0$ remain. The figure clarifies how the characteristic system approaches to its saturation magnetization with the increase of H.

V. CONCLUSIONS

In this work, we have investigated the field dependence of magnetization on the surface in the semi-infinite spin-$\frac{1}{2}$ Ising ferromagnet with a (100) uniform surface or a surface amorphization by the use of the effective-field theory corresponding to the Zernike approximation in the bulk. The obtained results have revealed some characteristic behaviors of magnetism at the surfaces.

In Sec. II, the magnetization processes of surface and bulk magnetizations for the system with a (100) uniform surface have shown some differences, depending on whether Δ_s is larger or smaller than a critical value Δ_c. In particular, the Arrott plots at the surface ordering temperature show big differences, depending on whether σ_s^2 is plotted as a function of $H/J\sigma_s$ or H/J_{σ_B}, as shown in Fig. 5. From these differences, the existence of surface magnetic ordering may be confirmed experimentally, especially in the temperature range above the bulk Curie temperature.

In Sec. IV, we have examined the field dependence of surface magnetization for the system with an amorphous surface layer in relation to the characteristic behavior found in previous work.[9] The results also indicate that the study of a surface with an amorphous layer in an applied field is extremely interesting.

As mentioned before, we have used in this work the effective-field theory corresponding to the Zernike approximation in the bulk. In the approximation we have decoupled multispin correlation functions $\langle S_i^z S_j^z \cdots S_k^z \rangle$ into $\langle S_i^z \rangle \langle S_j^z \rangle \cdots \langle S_k^z \rangle$ (see Refs. 7 and 15). The decoupling simply corresponds to the Zernike approximation in the bulk.[11] But it improves the results obtained from the standard mean-field theory in a reasonable direction. Especially, the application to the surface magnetic problem is superior to that of the standard mean-field theory, as discussed in detail in a review article.[18] Moreover, we can improve the decoupling approximation by introducing the concept of a correlated effective field and a new decoupling approximation into the multispin correlation functions. The improved theories give the results equivalent or superior to those of Bethe-Peierls approximation. However, the approximations to the surface magnetic problems become more complicated than that of the present framework, as discussed in Ref. 19.

Finally, we hope that our study will stimulate further experimental and theoretical works on the systems considered here. A comparison of our work with experiment should be worthwhile.

APPENDIX

The coefficients A_i $(i=1-10)$, B_i $(i=1-12)$, and K_i $(i=1-7)$ of Eqs. (6), (7), and (8) are given by

$$
\begin{aligned}
A_1&=(C_s)^4C_1f(x)|_{x=0}\,,\\
A_2&=(C_s)^3S_sC_1f(x)|_{x=0}\,,\\
A_3&=(C_s)^2(S_s)^2C_1f(x)|_{x=0}\,,\\
A_4&=C_s(S_s)^3C_1f(x)|_{x=0}\,,\\
A_5&=(S_s)^4C_1f(x)|_{x=0}\,,\\
A_6&=(C_s)^4S_1f(x)|_{x=0}\,,\\
A_7&=(C_s)^3S_sS_1f(x)|_{x=0}\,,\\
A_8&=(C_s^2)(S_s)^2S_1f(x)|_{x=0}\,,\\
A_9&=C_s(S_s)^3S_1f(x)|_{x+0}\,,\\
A_{10}&=(S_s)^4S_1f(x)|_{x=0}\,,
\end{aligned}
\tag{A1}
$$

$$
\begin{aligned}
B_1 &= (C)^5 C_1 f(x)|_{x=0} , \\
B_2 &= (C)^4 S C_1 f(x)|_{x=0} , \\
B_3 &= (C)^3 (S)^2 C_1 f(x)|_{x=0} , \\
B_4 &= (C)^2 (S)^3 C_1 f(x)|_{x=0} , \\
B_5 &= C (S)^4 C_1 f(x)|_{x=0} , \\
B_6 &= (S)^4 C_1 f(x)|_{x=0} , \\
B_7 &= (C)^5 S_1 f(x)|_{x=0} , \\
B_8 &= (C)^4 S S_1 f(x)|_{x=0} , \\
B_9 &= (C)^3 (S)^2 S_1 f(x)|_{x=0} , \\
B_{10} &= (C)^2 (S)^3 S_1 f(x)|_{x=0} , \\
B_{11} &= C (S)^4 S_1 f(x)|_{x=0} , \\
B_{12} &= (S)^5 S_1 f(x)|_{x=0} ,
\end{aligned}
\tag{A2}
$$

and

$$
\begin{aligned}
K_1 &= (C)^6 f(x)|_{x=0} , \\
K_2 &(C)^5 S f(x)|_{x=0} , \\
K_3 &= (C)^4 (S)^2 f(x)|_{x=0} , \\
K_4 &= (C)^3 (S)^3 f(x)|_{x=0} , \\
K_5 &= (C)^2 (S)^4 f(x)|_{x=0} , \\
K_6 &= C (S)^5 f(x)_{x=0} , \\
K_7 &= (S)^6 f(x)|_{x=0} ,
\end{aligned}
\tag{A3}
$$

where parameters (C_s, S_s), $C_1, S_1)$, and (C, S) are defined by

$$
\begin{aligned}
C_s &= \langle \cosh(D\bar{J}_s) \rangle_r = \int P(\bar{J}_s) \cosh(D\bar{J}_s) d\bar{J}_s , \\
S_s &= \langle \sinh(D\bar{J}_s) \rangle_r = \int P(\bar{J}_s) \sinh(D\bar{J}_s) d\bar{J}_s ,
\end{aligned}
\tag{A4}
$$

$$
C_1 = \langle \cosh(D\bar{J}_1) \rangle_r ,
\tag{A5}
$$

$$
C_1 = \langle \cosh(D\bar{J}_1) \rangle_r ,
$$

and

$$
\begin{aligned}
C &= \cosh(DJ) , \\
S &= \sinh(DJ) .
\end{aligned}
\tag{A6}
$$

In Sec. III, the functions $P(\bar{J}_s)$ and $P(\bar{J}_1)$ are taken as $P(\bar{J}_s) = \delta(\bar{J}_s - J_s)$ and $P(\bar{J}_1) = \delta(\bar{J}_1 - J_1)$. In Sec. IV, the functions $P(\bar{J}_s)$ and $P(\bar{J}_1)$ are given by (13). Then, the coefficients A_i, B_i, and K_i can be easily calculated by using a mathematical relation $e^{\gamma D} f(x) = f(x + \gamma)$.

[1] D. L. Mills, Phys. Rev. B **3**, 387 (1971); **8**, 4424 (1973).
[2] K. Binder and P. C. Hohenberg, Phys. Rev. B **9**, 2194 (1974).
[3] K. Binder and D. P. Landau, Phys. Rev. Lett. **52**, 318 (1984).
[4] See the book, *Magnetic Properties of Low-Dimensional Systems*, edited by L. M. Falicov and J. L. Moran-Lopez (Springer-Verlag, Berlin, 1986).
[5] T. W. Burkhard and E. Eisenberger, Phys. Rev. B **16**, 3213 (1977).
[6] M. Wortis and N. M. Svarakic, IEEE Trans. Magn. **MAG-18**, 721 (1982).
[7] T. Kaneyoshi, I. Tamura, and E. F. Sarmento, Phys. Rev. B **28**, 6491 (1983).
[8] T. Wolfarm, R. E. Dwames, W. H. Hall, and P. W. Palmberg, Surf. Sci. **28**, 45 (1971).
[9] T. Kaneyoshi, Phys. Rev. B **39**, 557 (1989).
[10] T. Kaneyoshi, J. Phys. C **21**, 5259 (1988).
[11] F. Zernike, Physica (The Hague) **7**, 565 (1940).
[12] M. E. Fisher, Rep. Prog. Phys. **30**, 615 (1976).
[13] E. F. Sarmento and C. Tsallis, Phys. Rev. B **27**, 5784 (1983).
[14] See *Proceedings of the Fourth International Conference on Rapidly Quenched Metals, Sendai, 1981,* edited by T. Masumoto and K. Suzuki (Japan Institute of Metals, Sendai, 1982).
[15] T. Kaneyoshi, R. Honmura, I. Tamura, and E. F. Sarmento, Phys. Rev. B **29**, 5121 (1984); T. Kaneyoshi and H. Beyer, J. Phys. Soc. Jpn. **49**, 1306 (1980).
[16] K. Handrich, Phys. Status Solidi B **32**, K55 (1969).
[17] T. Kaneyoshi and I. Tamura, Solid State Commun. **51**, 67 (1984).
[18] T. Kaneyoshi, Rev. Solid State Sci. **2**, 39 (1988).
[19] I. Tamura, E. F. Sarmento, I. P. Fittipaldi, and T. Kaneyoshi, Phys. Status Solidi B **118**, 409 (1983).